Article

Green Vessel Scheduling with Weather Impact and Emission Control Area Consideration

Xin Wen [1], Qiong Chen [2,*], Yu-Qi Yin [3] and **Yui-yip Lau [4]**

[1] School of Economics & Management, Jiangsu University of Science & Technology, Zhenjiang 212100, China
[2] Navigation College, Jimei University, Xiamen 361021, China
[3] Logistics & E-Commerce College, Zhejiang Wanli University, Ningbo 315100, China
[4] Division of Business and Hospitality Management, College of Professional and Continuing Education, The Hong Kong Polytechnic University, Hong Kong, China
[*] Correspondence: qchen@jmu.edu.cn

Abstract: Emissions of maritime transport have been a critical research topic with the substantial growth in the global shipping industry, encompassing both the expansion of the world fleet and the increased distances it has been covering recently. The International Maritime Organization (IMO) has enforced some regulations to mitigate ship Greenhouse Gas (GHG) emissions, which affect vessels' operational practice, and further affect service reliability. In this paper, some compliance methods (two-speed strategy, fuel switching, and LNG) against Emission Control Areas (ECAs) at the operational level are examined regarding if and how they impact the liner shipping schedule and service reliability; meanwhile, uncertain weather conditions and port times, as the main uncertain factors, are also involved. Then, a bi-objective fuzzy programming model is formulated and solved by the augmented ε-constraint approach, which generates a set of Pareto solutions by balancing the economic and environmental sustainability. Some findings can be concluded through the experimental results, including that, firstly, to meet uncertain weather conditions at sea requires strong robustness; secondly, ECA regulations can negatively affect the liner shipping service level; moreover, slow steaming is an immediate and effective measure to reduce GHG emissions; and, furthermore, ship routing choice could have a significant influence on ship emissions and service reliability.

Keywords: ship scheduling; speed optimization; emission control area; weather impact; fuzzy programming

MSC: 90-05; 90-10

1. Introduction

Shipping emissions have become an urgent concern for the IMO across recent decades up to now [1]. As ocean shipping is the backbone of global trade and heavily depends on fossil fuel, which mainly produces carbon emissions, GHG emissions are not supposed to be ignored as a portion of marine pollution. Unlike defining ECAs to limit sulfur and nitrogen emissions, international regulations to control carbon emissions are springing up, which involve technical and operational aspects, and further affect the efficient implementation into practice.

The rising volume in global trade has inevitably been causing an increase in GHG emissions. The IMO has introduced a series of mandatory measures technically and operationally against outputting GHG emissions. Newly built ships have been obliged to acquire a distinct "Energy Efficiency Design Index" (EEDI) via a technical approach. However, it is difficult to degrade engine power by sacrificing navigational safety and economic feasibility in practice [2]. Moreover, the Ship Energy Efficiency Management Plan (SEEMP) has been implemented at a practical level for liner shipping operators. On 13 April 2018, the IMO officially committed to slashing the total annual GHG emissions

from sea transportation by at least 50% by 2050 in contrast with 2008, which marks the launch of the first concerted mitigation goal [3]. The EEXI (Energy Efficiency Existing Ship Index) was introduced in MARPOL Annex VI in 2022 as a mandatory technical provision suitable for existing ships, and the CII (Carbon Intensity Indicator) has been put into force for vessels over 5000 tons since 2023. To curb sulfur emissions, the IMO has nominated four "Sulphur Emission Control Areas" (ECAs) to enforce limitations on sulfur oxides (SO_x) [4]. Ship operators have to switch to low-sulfur fuel to achieve compliance with these regulations, whereas the low-sulfur fuels (e.g., low-sulfur HFO (LSHFO), marine gas oil (MGO), marine diesel oil (MDO), and liquefied natural gas (LNG)) used inside the ECA have higher prices than the ordinary heavy fuel oil (HFO) utilized outside ECAs [2]. Sometimes, fuel costs from some types of ships have accounted for about 50–60% of the total operating costs [5,6] as the major component in the shipping costs. There is no doubt that the increasing attention paid to environmental benefits also affects shipping operations and sustainability.

Service performance is also vital for shipping lines in terms of creating vessel schedules. During maritime transportation, various uncertain factors lead vessels to deviate from their planned timetable. CargoSmart reports that 49% of 587 vessels' arrivals at US and South American ports were delayed from the planned schedule [7]. A detailed shipper satisfaction survey reveals that, quality of customer service and the reliability of transit times and booking/cargo shipments garnered scores ranging between 2.9 and 3 (from 1, very dissatisfied to 5, very satisfied) [8]. We will undertake deep consideration of regular uncertainties, which are classified into two categories [9]. One type is uncertainty at sea, namely the ocean environment, which includes wind, waves, current, and tide. Particularly adverse weather conditions in the winter season, as a main uncertain factor, will impact speeds and times spent on sailing and service. Fuel consumption and ensuing emissions produce an increase in high waves. Another type is uncertainty at the port, involving port congestion, variation in the number of handled containers, insufficient equipment capability, and unexpected waiting time for navigation. Uncertainties will impact schedule reliability and environmental performance, especially when schedules are not designed very well.

This paper considers the green vessel scheduling problem while accounting for restrictions on uncertainties and ECA regulations. To hedge against uncertainties at sea and ports, it is highlighted that a service schedule with uncertain weather conditions and fuzzy handling volume at a certain service level is generated, which also fills the research gap pertaining to the current studies. A novel bi-objective model and fuzzy programming approach are developed to analyze the conflicting objectives, which not only introduces ECA regulations but also captures robust weather conditions at sea and fuzzy port times. To develop an energy-efficient schedule, we undertake collective tactical planning to determine the number of deployed vessels, the sailing speeds, the ship routing, and the service schedule for environmental sustainability. The fuel switching strategy is recommended to examine whether ECA regulations impact operational measures, like fleet deployment and sailing patterns, and economic and service performances.

The remainder of this study is constructed in detail as indicated below. Section 2 provides a survey of the relevant studies on liner shipping service schedules, including speed models for reducing carbon emissions (Section 2.1), container shipping service with uncertain factors (Section 2.2), and the impacts of ECAs (Section 2.3). Section 3 describes the green ship scheduling problem considering uncertainties and ECA impact. Furthermore, the bi-objective model is presented for the problem. Section 4 confers the solution techniques utilized in this paper, while Section 5 establishes a series of experimental cases and sensitivity analyses to assess the performance of the formulated modeling. Finally, the findings and some concluding remarks are included.

2. Literature Review

There is a wide range of research carried out on ocean container transport, which can be categorized into three main classes: strategic decisions, tactical decisions, and operational decisions [10]. The ship scheduling and slow steaming problems belong to the tactical decision category in medium-term planning. Since fuel consumption is nonlinearly related to sailing speed and ship emissions are directly proportional to fuel burned, a recent trend in container transport has turned to sailing speed to capture environmental issues [11]. Therefore, a change in speed can dramatically impact both ship fuel consumption and emissions.

2.1. Liner Ship Scheduling under Carbon Emissions

Among extensive studies on the subject of vessel scheduling models, much fewer have investigated this problem on both operational and environmental aspects (i.e., "green vessel scheduling"). Fagerholt et al. [12] study the fuel consumption function of speed as a nonlinear continuous program, first discretizing the arrival times with a time window and then applying the shortest path method to solve it. Based on their studies, Norstad et al. [13] and Hvattum et al. [14] further develop different algorithms to solve the same problem, subjecting to fixed time windows with a satisfying 100% service level. Considering the speed optimization problem with transshipment and container routing, Wang and Meng [15] establish a mixed-integer nonlinear model, which is solved by the outer approximation algorithm. Wang et al. [16] identify a port that can be visited more than once, which extends their previous research. Alharbi et al. [17] remodel it as an integer linear optimization formulation, solving by the proposed iterative method. Zheng et al. [18] consider the service frequency restrictions in the ship deployment and speed optimization problem. Wu et al. [19] explore the influence of EEOIs on solving ship deployment, sailing speed, and routing choice problems. Alex et al. [20] explore the emissions, associated contaminants, and public health implications of exposure to road-dust-associated viruses to identify that road dust really participates in viral transmission.

The above-reviewed literature proves that the current tendencies in maritime transportation have paid attention to speed strategies and environmental concerns regarding ships. Recent research on this topic has addressed the schedule reliability concern in liner shipping. However, the above studies on carbon emissions considering uncertain factors are limited; particularly, they do not consider the impact of weather.

2.2. Liner Ship Scheduling under Uncertainty

Uncertainty is an important characteristic of maritime transportation. For the sake of improving service effectiveness, it is essential to think about mitigating the impact of uncertainties rather than merely addressing economic and environmental concerns. The causes of vessel delays or earliness are commonly classified into two groups [21]. The first includes uncertainties that occur frequently, like port/terminal congestion, accidental waiting period during berthing or mooring, insufficient port/terminal productivity, accidental waiting period at port-channel access (pilotage or towage), mechanical failures, and bad weather. The second refers to an irregular or one-off event, like labor strikes. Here, we just focus on regular uncertainties.

The literature addressing fuel consumption with uncertainties at sea and or/and at ports is very limited. Qi and Song [22] deal with the vessel schedule problem regarding the impact of uncertain port times by introducing the penalty of vessel delays, which aims to decrease the total fuel consumption while sustaining different service levels. They designed a robust containership route schedule to hedge against uncertain wait times and container handling times, which allows fast steaming to recover the delayed schedule and seek to obtain a trade-off between buffer time and schedule robustness. Wang and Meng [9] explore the optimal containership schedule design problem by capturing uncertain factors at sea and ports. A mixed-integer nonlinear stochastic programming model is proposed, aiming to minimize the shipping cost and expected fuel cost in the presence of a

certain transit time service level and no ship delays. Song et al. [23] formulate a stochastic multi-objective model for the joint tactical planning of vessel scheduling problems. The model aims to obtain the non-dominated relationship between the three objectives of minimizing total operating costs, service reliability, and shipping emission subject to port time uncertainty. Aydin et al. [24] present a dynamic programming model for speed optimization to minimize total fuel consumption by discretizing port arrival times with stochastic port times while maintaining schedule reliability. Dulebenets [25] develops a novel mixed-integer nonlinear mathematical model to improve vessel schedule planning and energy efficiency by regarding the carbon dioxide emission costs at sea and ports of call. Only Wang and Meng [15] refer to uncertainty at sea among the mentioned studies above, whilst most papers just take into account uncertainty at ports. However, the weather conditions at sea need to be considered as an important uncertain factor when shipping operators plan for vessel schedules.

Norlund et al. [26] develop a simulation-optimization-based methodology for generating a weekly supply vessel schedule, which incorporates both costs and emission reductions subject to different degrees of robustness. Norlund and Gribkovskaia [27] propose a simulation-optimization approach to minimize the total fuel consumption for week-frequency vessel schedules in different weather conditions. They both take into account changing weather conditions for speed optimization and estimating fuel consumption. The weather is modeled as a Markov chain in their papers, and we will refer to this assumption in this paper.

Mulder and Dekker [28] model the ship delay recovery problem as a Markov decision process to determine the optimal recovery policy and buffer time allocation by minimizing the total costs. Wen et al. [29] study dynamic recovery policies for liner shipping service with the consideration of buffer time allocation and uncertainties. Some new methods to solve uncertainties are proposed in decisionmaking. Debnath and Roy [30] apply an emerging tool, T-spherical fuzzy set (T-SFS), to deal with uncertainty and solve hydrogen (H2) refueling station site selection. Mondal et al. [31] put forward a novel three-way multi-attribute decisionmaking model under an incomplete information system. The above updated references study recovery polices or strategies to alleviate uncertainties.

2.3. Liner Ship Scheduling under ECA Impact

International shipping, as one of the more environmentally friendly transportation modes, still produces substantial emissions as a result of burning fuels. The IMO has enforced several regulations on ships moving between different jurisdictions; e.g., they have imposed strict limits on the maximum sulfur content for ships in the ECA. By complying with ECA sulfur regulations, shipping lines mainly adopt three methods, including fuel switching, utilizing LNG as a substitute, or installing a scrubber [5,12].

By minimizing operating costs, Fagerholt et al. [5] formulate an optimization model to determine the sailing pattern, including route and speed decisions. The motivation is to evaluate the consequences of these decisions and fuel consumption regarding ECA regulations. Fagerholt and Psaraftis [32] consider the strict limits on sulfur emissions to optimize two speeds for ships sailing in and out of the ECA by maximizing daily profit, which also involves the ECA refraction problem optimizing the point at the ECA boundary. Gu and Wallace [33] evaluate and select sulfur abatement technology (fuel switching, using LNG, or installing a scrubber) to meet the newest ECA rules. The research aims to analyze the implication of ships' sailing mode with different ECA compliance measures for the global environment. The former two papers only switch to lower sulfur for ships when sailing inside the ECA, while Gu and Wallace [33] compare three technologies under ECA limits and indicate that the scrubber system is more suitable for more ECA port calls on the shipping trade line. As the scrubber system is not effective for carbon reduction, we discuss fuel switching and using LNG as an alternative. Dulebenets [25] introduces both emission restrictions within the ECA and cargo transit time concerns for the green ship scheduling

problem. They formulate a mixed-integer nonlinear mathematical programming model, which aims to minimize the total route service cost.

There are also some papers studying whether and how the ECA regulations impact other areas of shipping operations. Lindstad et al. [34] assess costs and fuel consumption as a function of emission reduction options in ECAs while not involving port-side consequences. Chang et al. [35] use a two-stage measure to explore whether ECA factors influence the efficiency of port operations in regulatory areas, whereas the results show that ECA regulations can cause efficiency loss in ports operating. Chen et al. [36] model route-choosing behaviors of liner shipping to investigate the effects of the ECA on global shipping, which reveals that a large number of ships will pass around the ECA; meanwhile, the regional emissions will exceed the standard if an ECA is established. Zhen et al. [37] construe the bi-objective model sailing inside and outside ECAs to optimize routing and speeds. Zhuge et al. [38] study the sulfur regulations, carbon tax, and incentive mechanism. However, the above studies examine the ECA regulations' impact but do not consider the weather impact at sea.

The highlights of this paper include threefold aspects. First of all, a novel bi-objective fuzzy programming model is formulated for the green containership scheduling problem regarding weather impact and ECAs, which aims to analyze the trade-off between environmental concerns and service reliability. Secondly, we introduce different weather conditions at sea and uncertain port times for the determining process of the sailing pattern, which maintains a required level of robustness with liner shipping schedule design. Thirdly, we present if and how different ECA compliance methods impact the two-speed strategy, even further influencing environmental sustainability and schedule reliability.

3. Problem Description and Model Formulation

In this part, we provide an academic expression. The research problem is described and the taxonomy is defined in Section 3.1. The configuration of the basic model with a cost-minimizing objective is explained in Section 3.2; meanwhile, the mathematical expression is provided. Section 3.3 provides the model formulation with maximizing service level.

3.1. Problem Description

Considering a universal liner shipping cooperation, a set of shipping lines are operated to provide weekly service at a fixed sequence of port calls. Differing from other shipping lines, liner shipping service is generally exemplified in its routines. Commonly, a fleet of vessels with identical types is arranged to visit each port on the shipping line more than one time, where a round-trip visit at each port of call is represented as a voyage. Vessels follow the preannounced schedule to sail through the shipping line in successive voyages, transferring containers at sea and loading/unloading containers at ports of call. Each voyage consists of legs between two ports, each leg is composed of two stretches inside and outside the ECA, and one stretch is separated by wave homogeneous regions due to wave forecasting data collected from China Marine Environmental Forecasting Center.

With the increasing environmental concerns implemented by the latest ECA regulation, a much more severe global sulfur emission cap since 2020 presents large opportunities for shipping manufacturing. How to choose the optimal compliance measure through alternatives is very important, to not only reduce GHG emissions but also evaluate schedule reliability. The first way is fuel switching, which means ships burn more common and cheaper types of fuel, heavy fuel oil (HFO) outside the ECA, while the marine gasoline oil (MGO) with a much higher price and lower than 0.1% sulfur will be utilized inside the ECA. Note that ultra-low-sulfur fuel oil (ULSFO) will be used outside the ECA to replace HFO, which contains 0.5% sulfur since 2020. The second option is using liquefied natural gas (LNG) as material for the ship's propulsion system. Although fuel switching only requires very limited initial investment and slight modifications to the ship, much heavier fuel costs for MGO and ULSFO need to be borne by ship owners. However, choosing

LNG can efficiently escape the high expense of MGO rather than assuming a large initial capital investment.

The green liner ship schedule problem under ECA limits is developed based on the traditional liner shipping service. We consider a two-speed strategy and different sailing route decisions with fuel switching inside and outside the ECA or LNG method. More specifically, the distances inside and outside the ECA are varying based on different sailing routes. The combined tactical planning problem for the number of vessels, the two sailing speeds on each leg, the sailing route, and the service schedule throughout the whole voyage will be determined. This paper aims to examine if and how the ECA compliance methods impact the liner shipping schedule and service reliability of liner shipping companies and ports, subject to uncertain weather conditions and uncertain port times. For depicting the dynamics of the scheme, the process when a ship leaves from port p to arrive at port p' is divided into three periods: sailing inside ECA, sailing outside ECA, and handling at port, as shown in Figure 1.
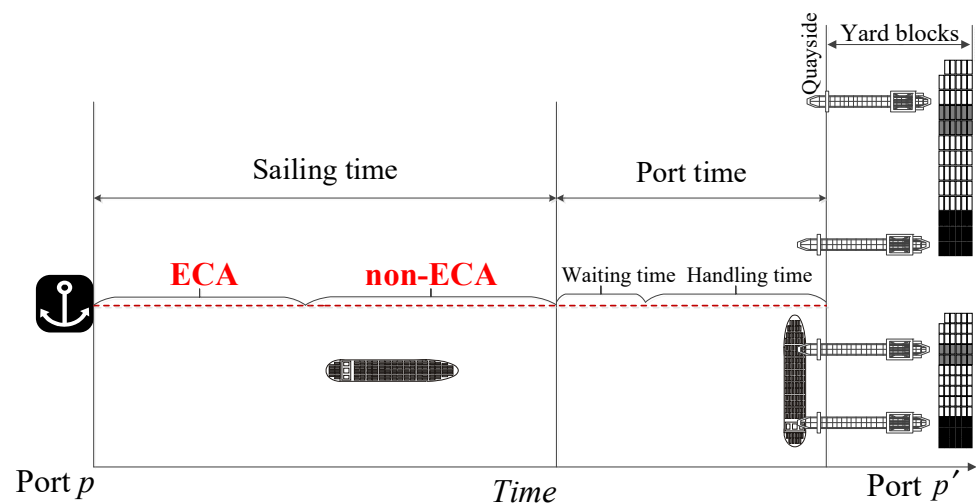

Figure 1. Dynamics of the liner shipping service inside and outside ECA.

3.2. Cost-Minimizing Model

Based on the problem description and assumptions above, we introduce nomenclature and notations, shown in Nomenclature part, to formulate the basic model of the green liner shipping schedule.

Referring to Figure 1, $\lambda = 1, 2$ indicates sailing periods inside and outside the ECA, respectively. Meanwhile, d_p^λ represents distances from port p to the next port inside and outside ECA when $\lambda = 1, 2$, varying with different sailing routes. $l \in L_p^\lambda$ expresses separate segments by different wave homogeneous regions, induced from wave forecasting data by China Marine Environmental Forecasting Center. Furthermore, Δv_l indicates the speed decrease on each segment $l \in L_p^\lambda$, which is produced following the Markov chain, according to varying weather conditions. The quantity of arranged vessels, the actual arrival and departure times, the sailing speeds inside and outside ECA on each leg, and the shipping route will be determined through the model.

The first objective aims to minimize the total costs for the shipping company, which consist of the fuel consumption cost, carbon emission tax, operating cost during the planning period, and handling activities cost. This decision-making process heavily depends on the implementation of cooperation and information sharing between shipping liners and ports. Equation (1) is the cost-minimizing objective, composed of Equations (2)–(5).

Namely,

$$\textbf{Min } F1 = FC + EC + OC + HC \tag{1}$$

$$FC = \sum_{k \in K} \sum_{l \in L} \sum_{p \in P} \sum_{\lambda \in \Lambda} \sum_{\delta \in S} f^{\lambda} \gamma_l^{\delta} v_{pk}^{\lambda \delta} + \sum_{k \in K} \sum_{p \in P} f^{MGO} \gamma^{port} t_{pk}^{port} \tag{2}$$

$$EC = \sum_{k \in K} \sum_{l \in L} \sum_{p \in P} \sum_{\lambda \in \Lambda} \sum_{\delta \in S} e^{\lambda} \theta^{\lambda} \gamma_l^{\delta} v_{pk}^{\lambda \delta} + \sum_{k \in K} \sum_{p \in P} e^{port} \theta^{port} \gamma^{port} t_{pk}^{port} \tag{3}$$

$$OC = nMT/24 \cdot u^o \tag{4}$$

$$HC = \sum_{k \in K} \sum_{p \in P} u^h \cdot h_{pk}/r_p \tag{5}$$

Subject to:

$$T = 168 \cdot n \tag{6}$$

$$T = \sum_{p \in P} \tau_p \tag{7}$$

$$\tau_p \geq h_p + \sum_{\lambda \in \Lambda} d_p^{\lambda}/s \qquad \forall\, p \in P \tag{8}$$

$$EAT_{pk} = (k-1)T + \sum_{j=1}^{p-1} \tau_j \qquad \forall\, p \in P,\, k \in K \tag{9}$$

$$EAT_{1,k} = EAT_{N+1,k} \qquad \forall\, k \in K \tag{10}$$

$$EAT_{1,1} = A_{1,1} \tag{11}$$

$$EDT_{pk} = EAT_{pk} + h_{pk}/r_p \qquad \forall\, p \in P,\, k \in K \tag{12}$$

Constraint (6) maintains the shipping service with weekly frequency [9]. Constraints (7)–(11) ensure the regularity and consistency of the container shipping service [23]. Constraint (12) represents the minimum expected departure time.

$$A_{1,k} = D_{N,k-1} + t_{N,k-1}^{sailing} \qquad \forall\, k \in [2,3,\dots M] \tag{13}$$

$$A_{p,k} = D_{p-1,k} + t_{p-1,k}^{sailing} \qquad \forall\, p \in [2,3,\dots,N],\, k \in K \tag{14}$$

Equations (13) and (14) represent the actual arrival times along the voyage. In detail, Equation (13) restricts the actual arrival times at the origin port on the following voyages except for the first one, while the arrival times at the following ports when $p \in [2,3,\dots,N], k \in K$ are imposed as Equation (14).

$$t_{p,k}^{sailing} = \sum_{\lambda \in \Lambda} \sum_{\delta \in S} \Delta^{\delta} d_p^{\lambda} v_{pk}^{\lambda \delta} \qquad \forall\, p \in P,\, k \in K \tag{15}$$

The sailing time is linearized through discretizing sailing speeds as Equation (15).

$$D_{p,k} = A_{p,k} + t_{pk}^{port} \qquad \forall\, p \in P,\, k \in K \tag{16}$$

Equation (16) endogenously denotes the dynamics after saving at the port, which, plus the port time, then turns into the departure time.

$$t_{pk}^{port} = \xi_{pk} + h_{pk}/r_p \qquad \forall\, p \in P,\, k \in K \tag{17}$$

Equation (17) represents that the total port time is the operating time plus the uncertain part at the port.

$$\gamma_l^\delta = \frac{\left(\frac{\delta}{s}\right)^3 f_s d_l}{\delta - \Delta v_l} \qquad\qquad \forall\, \delta \in S, l \in L_p^\lambda \qquad (18)$$

In Equation (18), the fuel consumption for each segment $l \in L_p^\lambda$ is measured in tons and developed based on the realistic closed-form approximation of fuel consumption [4]. In addition, this fuel consumption function takes into account the uncertain weather conditions, referring to Norlund et al. [26], given the assumption that the engine power output would not alter under different weather conditions. Severe weather conditions will augment resistance to cause speed reduction, while the unit fuel consumption remains unchanged. Then, the sailing time for a given instance rises owing to extra resistance, where Δv_l is the speed reduction due to wave height varying on different segments $l \in L_p^\lambda$. Each weather state highly depends on the previous state and may change every 6 h.

$$\sum_{\delta \in S} v_{pk}^{\lambda\delta} = 1 \qquad\qquad \forall\, \lambda \in \Lambda, p \in P, k \in K \qquad (19)$$

Equation (19) ensures that one speed from the speed bracket is selected on each stretch within or outside ECA on each leg.

$$v_{pk}^{\lambda\delta} \in \{0, 1\} \qquad\qquad \forall\, \delta \in S, \lambda \in \Lambda, p \in P, k \in K \qquad (20)$$

$$\tau_p \in R^+ \qquad\qquad \forall\, p \in P \qquad (21)$$

$$T \in Z^+, \; n \in Z^+ \qquad (22)$$

$$A_{pk} \in Q^+, \; D_{pk} \in Q^+, \; t_{pk}^{sailing} \in Q^+, \; t_{pk}^{port} \in Q^+, \; w_{pk} \in Q \qquad\qquad \forall\, p \in P, k \in K \quad (23)$$

$$\gamma_l^\delta \in R^+ \qquad\qquad \forall\, \delta \in S, l \in L_p^\lambda \qquad (24)$$

Equations (20)–(24) impose the nature and domains for all the decision variables.

3.2.1. Uncertain Weather Conditions

The sea environment involves waves, wind, and currents as some of the key factors, which significantly impacts ship route planning to follow the published schedule, which affects both sailing and service times. When ships travel at sea, the sailing speed will decline because of the impacts of wind and wave resistance. The above phenomenon represents so-called speed loss, not only linking to ship tonnage, draught, and hull shape but also relying on attributes of cargo and stowage. The planners of liner shipping service regard wave height as the most vital weather cause as it impacts sailing duration and service time, and may result in waiting before entering the port because of safety requirements for the loading and unloading process. Especially in winter months, the waves are on average higher and larger, fluctuating more than in summer months. The period of a voyage in winter will normally be longer than that in summer.

In this paper, the impact of waves on ship speed and ship exhaust emissions is analyzed and mathematically modeled. Uncertainty and robustness of wave height information are integrated to identify ship activities exactly. Involving robustness concerns in a schedule may lead to the application of additional vessels because of longer voyages, which impacts the costs, fuel, consumption, and emissions forwardly.

Referring to Norlund et al. [26], we take into account the environment robustness parameter η, which represents the robust level of wave state when making the schedule and takes the value in $[0, 1]$. Then, we assume that the wave heights in a fixed period are extremely relying on those in the earlier period following the Markov process, and the wave height changes dynamically per 6 h time due to wave forecasting data [39]. The weather statuses with the corresponding impacts on sailing speed are shown in Table 1, where the loss in sailing speed is assumed in a reasonable range. Furthermore, the probability distribution of weather conditions is discretized and set as $P = [p_1, p_2, p_3, p_4]$, where p_1 represents the weather state 1 when speed loss is 0 kts and p_2 includes states 1 and 2. Similarly, p_3 denotes speed loss is 0–3.5 kts; p_4 consists of the first four states; and '1' represents all the states that are possible to appear.

Table 1. Weather status.

Weather Status	Distinct Wave Height (m)	Loss in Sailing Speed (kts)
1	<1.5	0
2	[1.5, 2.5)	1
3	[2.5, 3.5)	2
4	[3.5, 4.5)	3
5	[4.5, 8)	4

Based on these assumptions, we calculate the average speed loss on each segment $l \in L_p^\lambda$. The pseudo-code for the production of Δv_l is shown in Table 2, where η_l indicates the robust level of wave heights on each segment, $X_l^{(t)}$ indicates the weather condition in tth period, and EAT_l represents the expected arrival time when the vessel sails to segment l. Then, $X_l^{(0)}$ iterate according to Markov transition matrices $\Phi = [\Phi_1, \Phi_2, \Phi_3, \Phi_4, \Phi_5]$ till the segment ends.

Table 2. Pseudo-code for the production of the speed decrease.

```
set robust level η_l in [0, 1]
if η_l ∈ [0, p_1] do
    X_l^(1) = Φ_1 X_l^(0) generate Δv_l = 0 then
    else if η_l ∈ (p_1, p_2] do
    X_l^(1) = Φ_2 X_l^(0) generate Δv_l = [0, 1]
    else if η_l ∈ (p_2, p_3] do
    X_l^(1) = Φ_3 X_l^(0) generate Δv_l = [0, 1, 2]
    else if η_l ∈ (p_3, p_4] do
    X_l^(1) = Φ_4 X_l^(0) generate Δv_l = [0, 1, 2, 3]
    else if η_l ∈ (p_4, 1] do
    X_l^(1) = Φ_5 X_l^(0) generate Δv_l = [0, 1, 2, 3, 4]
    then iterate
            if Iteration Number = ⌊EAT_l/6⌋
            end if
end if
```

3.2.2. Uncertain Port Times—ME Measure

The *ME* measure is introduced by referring to Xu and Zhou [40], which is proper for real-life decision-making problems in fuzzy circumstances. Then, a general fuzzy bi-objective model is established with expected objectives and chance constraints (ECM) subject to the *ME*. The loading and unloading operation times face a complex environment, including deviation in arrival time, inefficient berth allocation plan, mechanical failure or maintenance, port congestion, and other unforeseen events. Considering the uncertain handling times as fuzzy parameters, the basic model with objective functions and constraints is converted into its crisp counterparts based on the *ME* measure.

Firstly, a tight style of the basic possibility chance-constraint programming formulation is as below, where the expected value of *HC* is denoted as $E[HC]$ and transformed from constraint (17). The uncertain parameter of handling volume is presented as a triangular fuzzy variable: $\tilde{h}_{pk} = \left(h_{pk}, \alpha_{pk}, \beta_{pk} \right)$. σ_{pk} indicates the minimum confidence level, which is assumed to be satisfied with by the chance constraints.

$$\textbf{Min}\ \ E[F1] = E[FC + EC + OC + HC] = FC + EC + OC + E[HC]$$

s.t.

$$Me\left\{ \left(t_{pk}^{port} - \xi_{pk} \right) \cdot r_{pk} \geq \tilde{h}_{pk} \right\} \geq \sigma_{pk} \qquad \forall\, k \in K,\ p \in P \qquad (25)$$

Following Xu and Zhou [40], the aforementioned model can be converted into two models with the possibility of *Pos* and the necessity *Nec*. Specifically, the *Pos* measure stands for optimistic attitude, while the *Nec* measure stands for highly pessimistic attitude.

The lower approximation model (LAM) and the upper approximation model (UAM) are stated as listed below:

$$\textbf{Min}\ E[F1]$$

(LAM) s.t.

$$Nec\left\{ \left(t_{pk}^{port} - \xi_{pk} \right) \cdot r_{pk} \geq \tilde{h}_{pk} \right\} \geq \sigma_{pk} \qquad \forall\, k \in K,\ p \in P \qquad (26)$$

and

$$\textbf{Min}\ E[F1]$$

(UAM) s.t.

$$Pos\left\{ \left(t_{pk}^{port} - \xi_{pk} \right) \cdot r_{pk} \geq \tilde{h}_{pk} \right\} \geq \sigma_{pk} \qquad \forall\, k \in K,\ p \in P \qquad (27)$$

The crisp counterpart expression of the above models can be formulated by

$$\textbf{Min}E[F1] = \sum_{k \in K} \sum_{l \in L} \sum_{p \in P} \sum_{\lambda \in \Lambda} \sum_{\delta \in S} f^{\lambda} \gamma_l^{\delta} v_{pk}^{\lambda\delta} + \sum_{k \in K} \sum_{p \in P} f^{MGO} \gamma^{port} t_{pk}^{port}$$
$$+ \sum_{k \in K} \sum_{l \in L} \sum_{p \in P} \sum_{\lambda \in \Lambda} \sum_{\delta \in S} e^{\lambda} \theta^{\lambda} \gamma_l^{\delta} v_{pk}^{\lambda\delta} + \sum_{k \in K} \sum_{p \in P} e^{port} \theta^{port} \gamma^{port} t_{pk}^{port}$$
$$+ nMT/24 \cdot u^o$$
$$+ \sum_{k \in K} \sum_{p \in P} \left(\frac{1-\rho}{2} \left(h_{pk} - \alpha_{pk} \right) + \frac{h_{pk}}{2} + \frac{\rho}{2} \left(h_{pk} + \beta_{pk} \right) \right) u^h / r_p$$

(LAM) s.t.

$$\left(t_{pk}^{port} - \xi_{pk} \right) \cdot r_{pk} \geq h_{pk} + \left(1 - \sigma_{pk} \right) \cdot \beta_{pk} \qquad \forall\, k \in K,\ p \in P \qquad (28)$$

and

$$\textbf{Min}\ E[F1]$$

(UAM) s.t.

$$\left(t_{pk}^{port} - \xi_{pk} \right) \cdot r_{pk} \geq h_{pk} - \left(1 - \sigma_{pk} \right) \cdot \alpha_{pk} \qquad \forall\, k \in K,\ p \in P \qquad (29)$$

where $\rho(0 \leq \rho \leq 1)$ is the optimistic–pessimistic parameter to interpret the unified viewpoint of decisionmakers.

3.3. Service Level Maximizing Model

As referred to above, service level denotes a key aspect when designing vessel schedules by reliability [41,42]. The primary factor is uncertainties both at ports and at sea that exist in the voyage. The service level is determined by the most direct customers, shippers, or charterers. What customers mostly care about is whether they can receive their cargo on time or not; namely, schedule reliability is critical for customers. Nevertheless, if the schedule has been better-drafted considering uncertainties, it is available that the shipping line can acquire a higher service level at calling ports. Meanwhile, we also examine whether ECA regulations impact the efficiency of liner shipping service on the shipping routes through such areas.

The second objective aims to maximize the liner shipping service level or schedule reliability. The service level is generally measured using the delay time at the departure period, referring to Lee et al. [43] and Xiang et al. [44]. When a vessel arrives later than the contracted time window, customers' satisfaction starts to decrease. Since delayed cargo may lead to higher costs for customers, punctual delivery of containers plays a significant role in liner shipping service. Then, we can represent the increasing margin of delay impact as a stepwise function, where customers and ports along the maritime supply chain may bear a small delay, whilst a large delay will lead to deviation from the designed schedule and a negative impact on the service level.

This provides,

$$\mathbf{Max}\ F2 = \sum_{k \in K} \sum_{p \in P} w_{pk}\left(D_{pk} - EDT_{pk}\right) / (M \cdot N) \tag{30}$$

For busy ports:

$$w_{pk} = \begin{cases} 1 & if\ D_{pk} - EDT_{pk} \le 12 \\ 75\% & if\ 12 < D_{pk} - EDT_{pk} \le 24 \\ 50\% & if\ 24 < D_{pk} - EDT_{pk} \le 36 \\ 25\% & if\ 36 < D_{pk} - EDT_{pk} \le 48 \\ 0 & if\ D_{pk} - EDT_{pk} > 48 \end{cases} \qquad \forall\ p \in P, k \in K \tag{31}$$

For idle ports:

$$w_{pk} = \begin{cases} 1 & if\ D_{pk} - EDT_{pk} \le 16 \\ 80\% & if\ 16 < D_{pk} - EDT_{pk} \le 24 \\ 60\% & if\ 24 < D_{pk} - EDT_{pk} \le 36 \\ 40\% & if\ 36 < D_{pk} - EDT_{pk} \le 48 \\ 20\% & if\ 48 < D_{pk} - EDT_{pk} \le 60 \\ 0 & if\ D_{pk} - EDT_{pk} > 60 \end{cases} \qquad \forall\ p \in P, k \in K \tag{32}$$

So, we provide the bi-objective programming model, shown as Equations (1)–(24) and (28)–(32).

4. Solution Approach

Based on the possibilistic and fuzzy framework for modeling, it is, therefore, essential to propose the solution procedure for the complex problem. The model under an uncertain environment has already been defuzzified (i.e., transformed to its crisp counterpart) utilizing a new fuzzy method: *ME*.

In this section, the augmented epsilon-constraint measure [45] is applied to transform the bi-objective formulation into an equivalent single-objective model, which is a classic measure aiming to achieve optimal Pareto solutions.

The whole process of the proposed solution process is supplied in the subsequent steps:

Step 1: Apply the *ME* measure to convert the above model with fuzzy parameters into the basic possibilistic chance-constraint programming model by setting the minimum

confidence level, which is further transformed into two models with the possibility Pos and the necessity Nec. The conversion process is shown as Formulas (25)–(27).

Step 2: Defuzzify the resultant possibilistic objective function and constraints to their crisp counterpart formulation by using the optimistic–pessimistic parameter, shown as Formulas (28)–(29).

Step 3: Transform the bi-objective programming model after defuzzification by utilizing the augmented ε-constraint measure.

Step 4: Consider the minimum confidence level σ_{pk} and the optimistic–pessimistic parameter ρ according to the decisionmaker's preference, and then solve the proposed auxiliary crisp models (28)–(29).

Step 5: Restart *Steps* 1–4 to obtain the optimal compromise solution using an interactive measure with the decisionmaker until obtaining a satisfactory efficient compromise solution, where the interactive approach is implemented by varying control parameters, such as the weight vector of objectives, to achieve satisfaction [46].

The design of the augmented ε-constraint measure is explained in the following steps. Here, objective function (1): minimizing the total costs is considered as the main objective (33), while objective function (30): maximizing the service level is added to constraints (34)–(35), together complying with a feasible decision domain X. Specifically, an augmented term is introduced to ensure generating an effective resolution for each ε vector [47], where the ranges and priorities of objectives aim to normalize the augmented term while avoiding the scaling question; then, it can be turned into the following model:

$$\textbf{Min } \varphi_1 \frac{F_1(x) - F_1^{min}}{range_1} - \omega \cdot \varphi_2 \cdot \frac{s\mu_2}{range_2} \tag{33}$$

$$\text{s.t. } F_2(x) - s\mu_2 = \varepsilon_2 \tag{34}$$

$$x \in X; \; s\mu_2 \in R^+ \tag{35}$$

where φ_1 and φ_2 denote the priorities of these two objective functions and $\varphi_1 + \varphi_2 = 1$; ω denotes quite a small number (usually taking values in $[10^{-6}, 10^{-3}]$); $range_1$ and $range_2$ show the range of objective values; $s\mu_2$ represents the slack variable of the second objective. Furthermore, the varying Pareto solutions can be obtained by varying the ε vector, which is decided via the scope of every constrained objective function; meanwhile, the related payoff table can be filled.

Afterward, $range_p$ and ε_2 are further computed as following steps [45], where F_p^{max} and F_p^{min} represent the maximum and minimum values of objective p, correspondingly. Moreover, μ is the grid point's number and n_p are equal intervals that $range_p$ is divided into.

$$range_p = F_p^{max} - F_p^{min} \qquad \forall \, p = 1, 2 \tag{36}$$

$$\varepsilon_2^{\mu} = F_2^{max} - \frac{range_2}{n_2} \cdot \mu \qquad \forall \, \mu = 0, 1, \ldots, n_2 - 1 \tag{37}$$

Through the transformation, the bi-objective function is converted into the single function problem. All computational experiments in the following parts are implemented with ILOG CPLEX version 12.8, which is a powerful engineering computation software, by utilizing the branch-and-bound algorithm to solve the mixed-integer programming problem.

5. Numerical Experiments

In this part, the details of the experiments for the liner ship schedule design problem are offered to promote the performance of the extant schedule in the areas of cost efficiency, environment friendliness, and service reliability, and this is also conducted to validate the suggested solution to meet the uncertainties at sea and ports within the ECA restrictions.

5.1. Input Data Generation

Considering a trans-North Atlantic liner shipping service way [33], displayed in Table 3, it consists of seven ports (and eight ports of call), with ECA involvement in the string of GOT (Gothenburg, Sweden), HFX (Halifax, NS, Canada), NYK (New York, NY, USA), WTN (Wilmington, NC, USA), PCA (Canaveral, FL, USA), MIA (Miami, FL, USA), HOU (Houston, TX, USA), and back to GOT. Furthermore, different leg options are assigned in the loop with the same starting and ending ports, and then the sailing distances inside and outside the ECA as well as the total distances are different for route alternatives. Varying from Leg Option 0 to Leg Option 4, the path within the ECA gradually decreases whilst the total traveling distance increases. In other words, the ship sails the shortest total distance as well as sailing the longest distance in the ECA.

Table 3. Details of port calls in the shipping service and their route alternatives [33].

No.	Port	Handling Volume (*TEU*)	Distance (ECA/Non-ECA)—Nautical Miles				
			Option 0	Option 1	Option 2	Option 3	Option 4
1	Gothenburg	2500	1225/1635	1133/1938	848/2302	788/2517	664/2760
2	Halifax	2700	549/0	525/292	492/349	464/400	449/440
3	New York	3000	485/0	469/348	452/390	436/431	423/477
4	Wilmington	2300	361/0	298/254	287/265	276/282	265/348
5	Canaveral	2000	491/0	415/118	335/229	307/299	287/361
6	Miami	2100	641/0	565/171	467/303	413/400	397/465
7	Houston	2800	2422/2683	1586/3681	1257/4062	781/4610	661/4877

In our experiment, three voyages, i.e., $M = 3$, are considered, and four vessels of 8000~10,000 TEUs are assumed to be deployed to provide weekly service in the loop. The number of containers to be operated at every port is set as $U[2000, 3000]$ TEUs, and the handling rate is offered as $[100, 125]$ TEUs/h. In addition, the uncertainty of the ship's port time conforms to $N(24, 4.8^2)$ [23].

Furthermore, to evaluate the performance results under different weather conditions, we use the forecasting wave data in the North Atlantic from the China National Marine Environmental Forecasting Center (NMEFC) [39], as in Figure 2 (the ranges of latitude and longitude: N30~60, W100~E12). Referring to the significant wave heights both in the summer month of July and winter month of January, the start state probabilities and the transformation probabilities between each weather state for these two months are listed in Tables 4 and 5, respectively. The start state probabilities signify the occurring frequencies of the different weather statuses. Moreover, the transition matrices involve the possibilities, which indicate one weather stage in a time phase changing to another in the next time phase.

In the following, two sets of cases are presented. In the first group, the Pareto solutions of LAM and UAM models using the results are illustrated from the augmented ε-constraint method by changing σ_{pk}, ρ, and ε_2. More specifically, different solutions can be found with uncertain weather conditions and fuzzy handling volumes, which incur random port time. In the second group, the influence of important parameters is examined, involving the difference between ECA abatement options and sailing route alternatives. All computational experiments are implemented with CPLEX version 12.8 by utilizing a laptop with an Intel Core i5-6300HQ Processor (2.30 GHz) and 8 GB of RAM.

Table 4. Start state probabilities.

State 1	State 2	State 3	State 4	State 5
(a) July				
0.022	0.033	0.426	0.439	0.080
(b) January				
0.000	0.002	0.042	0.057	0.899

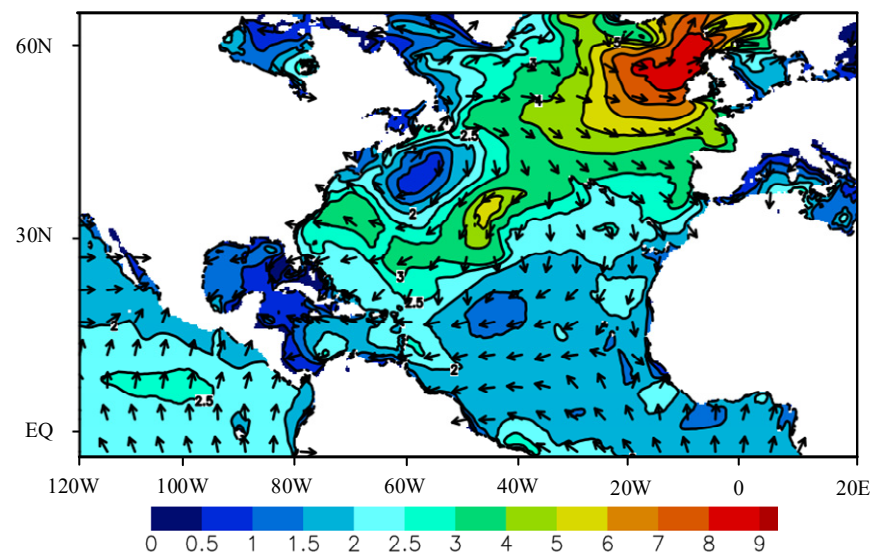**Figure 2.** Forecasting wave heights in North Atlantic.

Table 5. Transition matrices in summer and winter seasons.

	State 1	State 2	State 3	State 4	State 5
(a) July					
State 1	0.454	0.546	0.000	0.000	0.000
State 2	0.105	0.647	0.248	0.000	0.000
State 3	0.124	0.106	0.670	0.120	0.004
State 4	0.000	0.000	0.182	0.689	0.128
State 5	0.000	0.000	0.000	0.127	0.872
(b) January					
State 2	0.634	0.366	0.000	0.000	0.634
State 3	0.169	0.78	0.051	0.000	0.169
State 4	0.000	0.208	0.74	0.052	0.000
State 5	0.000	0.000	0.323	0.677	0.000

5.2. Solution Approach Performance

The experimental results are appraised for the deterministic model and fuzzy programming model. Different Pareto solutions are provided for variant combinations of confidence level $\sigma_{pk} = 0.8$, optimistic–pessimistic parameter $\rho = 0.5$, and ε_2. Here, we assume that route option 1 is provided in the loop under the abatement method; i.e., MGO and HFO are used inside and outside the ECA. The summer month of July is selected and the environment robustness parameter is assumed as $\eta = 0.5$. The triangular fuzzy numbers of handling volume vary by 50% based on the underlying values in Table 5. The cost-minimizing objective is considered as the main objective function, while the service-level-maximizing objective is regarded as a constraint while considering $\omega = 10^{-4}$, $\mu = 3$, $\varphi_1 = 0.5$, and $\varphi_2 = 0.5$. The other corresponding data according to the ships and service routes considered in the case study are provided in Table 6 as a situation in the shipping market.

Table 6. Input data settings.

Parameter	Value	Source(s)
Unit HFO cost: (USD/ton)	450	BunkerIndex [48]
Unit MGO cost: (USD/ton)	700	BunkerIndex [48]
Unit ULSFO cost: (USD/ton)	600	BunkerIndex [48]

Table 6. *Cont.*

Parameter	Value	Source(s)
Unit LNG cost: (USD/ton)	350	Lindstad et al. [34]
Carbon dioxide emission factor for HFO	3.13	IMO [1]
Carbon dioxide emission factor for MGO/MDO	3.19	Kontovas and Psaraftis [49]
Carbon dioxide emission factor for ULSFO	3.13	Kontovas and Psaraftis [49]
Carbon dioxide emission factor for LNG	2.75	Kontovas and Psaraftis [49]
Daily charter cost of large LNG ship (USD/day)	60,000	Clarkson [50]
Daily charter cost of 9000 TEU container vessel (USD/day)	35,000	Clarkson [50]
Handling cost (USD/h)	200	Venturini et al. [51]
Uncertain part of the port time (h)	$N(24, 4.8^2)$	Song et al. [23]
Handling rate (TEUs/h)	[100, 125]	Dulebenets [25]
Unit fuel consumption at port (ton/h)	0.35	Kontovas and Psaraftis [49]
Fuel consumption at the normal operational speed of 24 knots (ton/day)	250	Notteboom and Vernimmen [52]
Minimum sailing speed (knots)	14	Kontovas and Psaraftis [49]; Song et al. [23]
Maximum sailing speed (knots)	24	Kontovas and Psaraftis [49]; Song et al. [23]

5.2.1. Different ME Parameters

The results of the LAM and UAM models under different values of σ_{pk} (0.7 ∼ 1) and ρ (0 ∼ 1) are reported in Table 7.

Table 7. LAM and UAM results under different σ_{pk} and ρ.

ρ		0.7		0.8		0.9		1	
		obj1	obj2	obj1	obj2	obj1	obj2	obj1	obj2
0	LAM	12,605,710.444	0.7120	12,257,686.545	0.7209	11,948,331.726	0.7357	11,665,869.875	0.738
	UAM	10,896,004.011	0.8029	11,139,924.274	0.7723	11,395,660.072	0.7599	11,665,869.875	0.738
0.2	LAM	12,615,454.435	0.7123	12,267,430.537	0.7212	11,958,075.726	0.7360	11,675,613.847	0.7386
	UAM	10,906,138.331	0.8031	11,149,019.913	0.7726	11,405,750.050	0.7501	11,675,613.847	0.7386
0.4	LAM	12,625,198.423	0.7126	12,277,174.548	0.7214	11,967,819.726	0.7362	11,685,357.466	0.7386
	UAM	10,915,882.141	0.8031	11,158,763.901	0.7729	11,415,148.072	0.7504	11,685,357.466	0.7386
0.6	LAM	12,634,942.357	0.7126	12,286,918.457	0.7214	11,977,563.726	0.7362	11,695,101.387	0.7386
	UAM	10,925,626.314	0.8031	11,168,507.134	0.7729	11,424,892.072	0.7504	11,695,101.387	0.7386
0.8	LAM	12,644,686.766	0.7128	12,296,662.507	0.7216	11,987,307.726	0.7364	11,704,845.586	0.7388
	UAM	10,935,370.414	0.8033	11,178,263.436	0.7730	11,434,982.050	0.7506	11,704,845.586	0.7388
1	LAM	12,654,430.243	0.7131	12,306,406.702	0.7219	11,997,051.726	0.7367	11,714,589.365	0.7392
	UAM	10,945,114.633	0.8035	11,188,007.608	0.7732	11,444,380.072	0.7507	11,714,589.365	0.7392

To sum up, the feasible Pareto solutions according to the varying extent of optimistic–pessimistic parameters and confidence levels could be obtained through the proposed models and approaches since, in a fuzzy environment, crisp solutions from two proposed approximation models (LAM and UAM) provided to strategic decisionmakers are somehow unrealistic. As one of the main advantages of the ME measure, decisionmakers can obtain interval solutions in the fuzzifying procedure, and thus the upper and lower bounds for optimal solutions are provided, including more information [40].

Table 8 and Figure 3 illustrate the Pareto frontier of UAM by changing ε_2, which is realized with different μ and $\sigma_{pk} = 0.8, \rho = 0.5$. For this, the range of the second objective is calculated first, consisting of the best value of 0.973 and the nadir value of 0.214. It can be observed that the service level is improved with μ decreasing since a smaller μ provides a larger feasible region for the second objective in the constraint. As mentioned before, economic and service performances have contrary variation trends. The total cost is fairly sensitive at a lower service level compared to that at a higher service level. To improve service reliability, shipping lines need to speed up to cover the uncertainties at sea and ports, which incurs increases in fuel consumption and carbon emissions, and thus the corresponding costs.

Table 8. UAM results under alteration in μ $\left(\sigma_{pk} = 0.8, \rho = 0.5\right)$.

μ	obj1—Cost	obj2—Service Level
0	11,541,069.812407	0.9500
1	11,430,368.3133582	0.8927
2	11,272,543.7077613	0.8113
3	11,164,650.6703017	0.7735
4	11,076,200.8909524	0.7035
5	10,997,214.5430556	0.6743
6	10,931,762.8190744	0.6139
7	10,869,583.1940407	0.5002
8	10,806,026.4358411	0.4835
9	10,749,505.0545548	0.4522
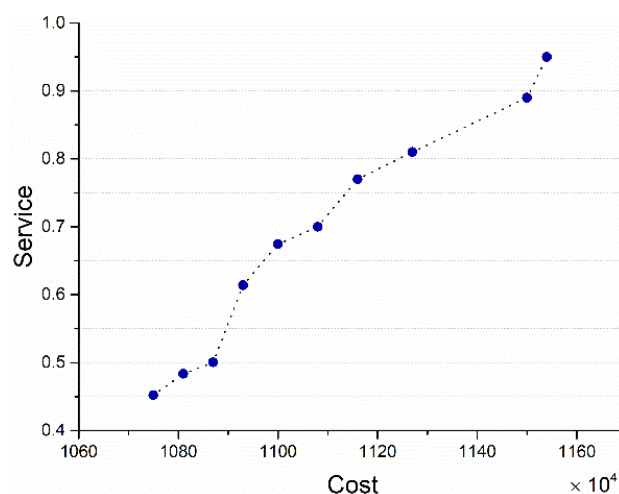
Figure 3. Pareto frontier of UAM under alteration in μ $\left(\sigma_{pk} = 0.8, \rho = 0.5\right)$.

5.2.2. Varying the Weather Robust Level η

Uncertain sea environments also have implications on the shipping lines' schedules. Added resistance due to adverse weather and sea conditions is mostly encountered in the ship journey. We will examine how such differentiation would affect sailing speed and port times.

In this experiment, considering $\mu = 5$, $\sigma_{pk} = 0.8$, and $\rho = 0.5$ on route option 1, we just account for the effect of wave reflection on added resistance without considering the wind effect to better illustrate how such differentiation in wave heights would impact fuel consumption and costs.

It can be seen that the cost objective value and its components, including the bunker consumption cost, carbon emission tax, and port service cost under different weather conditions, are represented in Figure 4. (i.e., I1~I5: different weather robust levels in July; I6~I9: different weather robust levels in January).

We observe that the total cost ranges from USD $10,817K$ $(10,816,694.5179)$ to USD $11,961K$ $(11,960,673.1524)$, while the service level stays around 67%. Some interesting aspects of the data can be observed. For both July and January, the cost value and corresponding components gradually increase with the robustness requirements increasing, which induces a decrease in speed and loss in fuel consumption. The cost rise is mainly related to the fuel consumption rise, which accounts for around two thirds of the total cost. The influence on cost and fuel consumption, considering the robustness requirements in a monotonous season, is quite bounded, even from strong robust sea environments. However, there cannot be a straightforward conclusion regarding the relationship between sea environments and speed strategy under the case settings. Even though the variation in wave heights causes a decrease in sailing speed, it does not affect the speed strategy of

decisionmakers considering cost minimization as the main objective. Another reason is that the adverse sea environment leads to an increase in sailing speed, which may also induce an increase in the number of deployed ships, rendering the speed strategies ineffective.
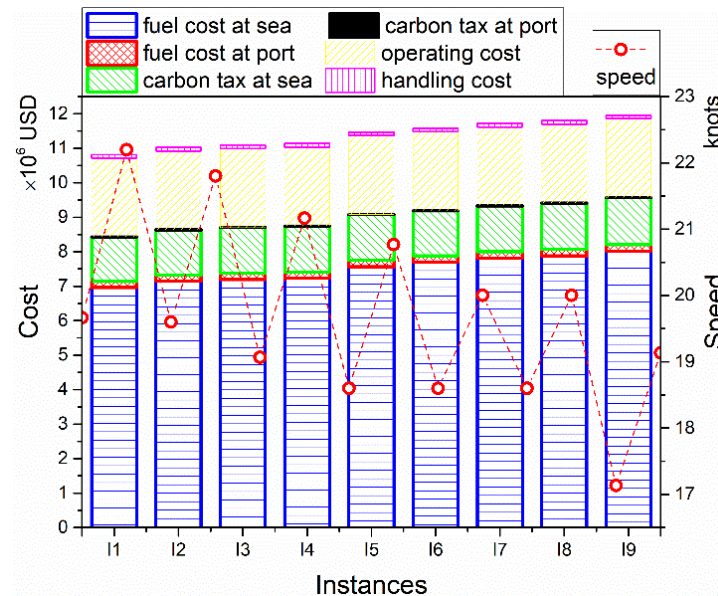

Figure 4. Objective functions, cost components, and average speed under weather in July and January.

We also represent the average speeds on seven legs inside and outside ECAs under nine instances, which have slight changes in different instances. The speed inside the ECA is higher than that outside the ECA due to the expensive bunker (MGO) selected to comply with the sulfur controls inside the ECA. When the ship sails on the leg with the longest distance, the speed reaches the lowest for bunker consumption saving. All the ships sail at high and medium speeds whether inside or outside the ECA because liner shipping companies and port operators need to maintain the service reliability at 67%, which is a constraint ($\mu = 5$), while minimizing the total cost.

5.2.3. Varying the Fuzzy Handling Volume

As in the above parameter settings, assume $\mu = 5$, $\sigma_{pk} = 0.8$, and $\rho = 0.5$ for route option 1. We vary the triangular fuzzy variable for the container handling volume with 20% increments from 10% to 90%, where the range 10% denotes that the fuzzy parameter varies 10% larger and smaller than the basic setting. The results are shown in Figures 5 and 6.

Similar patterns to Figure 4 can also be observed in Figure 5. The total cost and the components generally increase with the rise in handling volume and thus the container handling time. This could be caused when the vessel may speed up to maintain service reliability by saving sailing time, adding extra port time. The dramatic increase in bunker cost leads to the total cost rising. The operating cost and voyage time also increase, which can be explained in terms of the increased extent of port time being larger than the decreased extent of sailing time. A slight change in the container handling volume and further incurring a corresponding change in the port time have a moderate impact on the total cost. The service level decreases gradually from 68% to 64%, which is not plotted.

In addition, the achievement of differing speeds with port times increasing generally occurs, as shown in Figure 6. It shows that the sailing speed performs to be more related to the service unreliability with the consideration of port time rising when a vessel arrives late.
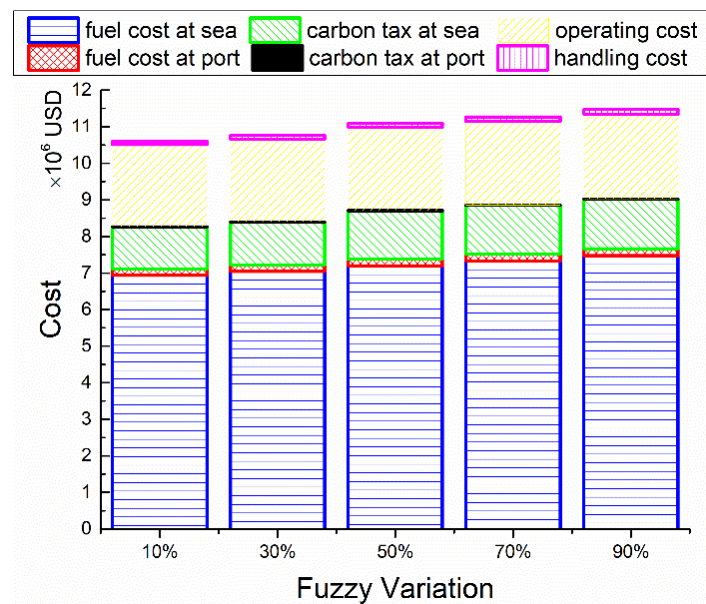
Figure 5. Objective functions and cost components accounting for fuzzy handling volume.
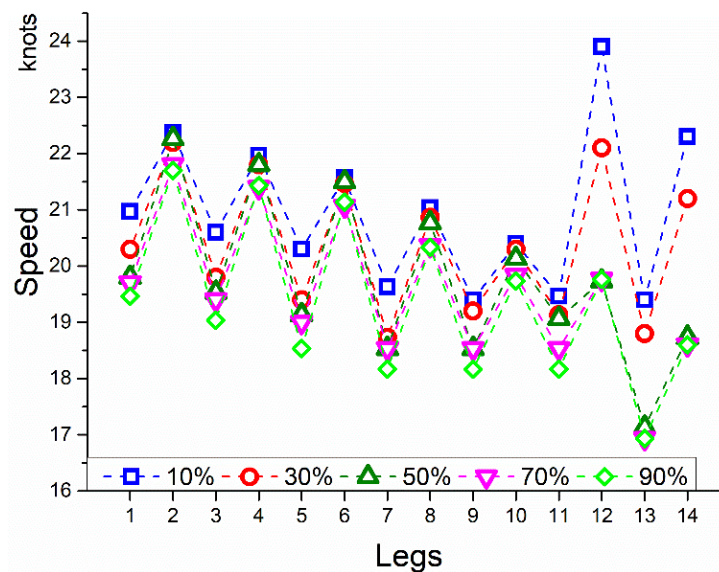

Figure 6. Average speed on each leg accounting for fuzzy handling volume.

5.3. Sensitivity Analysis

In this part, some managerial insights are provided, conducted on experimental examples regarding key parameters in the mathematical formulations.

5.3.1. Impacts of Different Abatement Alternatives

The fuel price has an impact on the experimental results, recognized as the key parameter. Accordingly, the sensitivity analysis is performed with different combinations of bunker prices corresponding to abatement alternatives.

Considering state 3 in July, $\sigma_{pk} = 0.8$, $\rho = 0.5$, and $\mu = 5$, we assume that the supply of LNG is sufficient. The daily chartering costs of a container ship and an LNG ship are set as USD 35 *K* and USD 60 *K*. We will present nine instances as follows: before 2020, MGO and HFO were used and set as (700, 450) USD/ton; after 2020, MGO and ULSFO are used and set as (700, 600), (700, 700), (800, 600), (900, 600), and (1000, 600) USD/ton. For the LNG case, it is set to be 350, 450, and 550 USD/ton.

Figure 7 shows the cost versus the service level of the Pareto solutions, as well as the carbon emissions in the bi-objective UAM models. Figure 8 shows the average speed on each leg under different instances. As can be observed from Figure 7, the total cost increases while the service level decreases with the bunker prices rising when the operating cost is fixed at USD 35*K*.
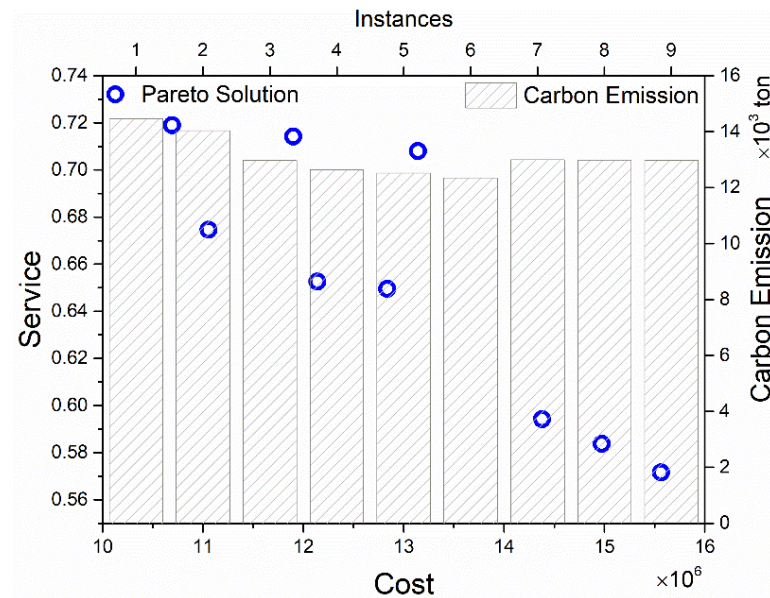

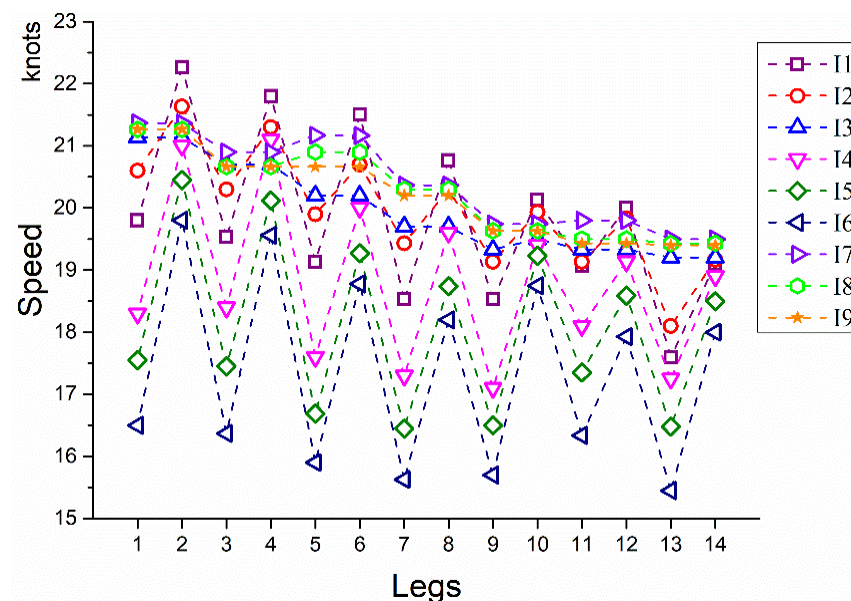**Figure 7.** Pareto solutions and carbon emissions under different abatement alternatives.

Figure 8. Average speed on each leg under different abatement alternatives.

As shown in Figure 8, the difference between two speeds inside and outside the ECA enlarges with the ratio of bunker prices increasing, and vice versa, by comparing instances 1–6. To be specific, the decline degree of speeds inside the ECA is larger than that outside the ECA. In addition, for the LNG cases in instances 7–9, ships sail above 19 knots, and it does not exist in two-speed conditions, where LNG can be used both inside and outside ECAs. Comparing all the Pareto solutions in Figure 8, when using LNG as substitute fuel, instances 7–9 show higher service levels in schedule design due to the lower price of LNG, and the carbon emissions approach to I3 with the bunker price (700, 700) USD/ton, while presenting higher than those in instances 7–9 and lower than those in instances 1–2.

However, the carbon emissions decrease with bunker price increasing in instances 1–6, the same as the trend in the total costs.

Finally, the varying Pareto solutions and speed decisions both show the importance of considering different abatement alternatives. LNG will be a better fuel alternative shortly, while MGO and ULSFO will not increase beyond a certain level, and the best solution in differing cases constantly presents a service-oriented schedule. Higher prices regarding MGO and ULSFO contribute to decreasing the fuel consumption and carbon emissions while raising the total cost and lowering the service level when taking ECA limits into account.

Furthermore, the experimental results depict that the liner shipping sector cannot meet the schedule reliability with a high service level, which results in additional fuel consumption and imposition of a carbon tax, which are relevant factors while considering economic benefits as the primary target.

5.3.2. Impacts of Different Shipping Routes

We also investigate the effect of different leg options (sailing routes and speed strategies) on the optimal solution. The shipping routes share the same origin and destination ports but vary the ECA, non-ECA, and total distances, as shown in Table 4. Assuming MGO (700 USD/ton) and HFO (450 USD/ton) are used and weather state 3 in July, $\sigma_{pk} = 0.5$, $\eta = 0.8$, and $\mu = 5$, Figure 9 illustrates the comparison of Pareto solutions and carbon emissions on different sailing routes. Figure 10 shows the speed strategy involving different sailing routes.
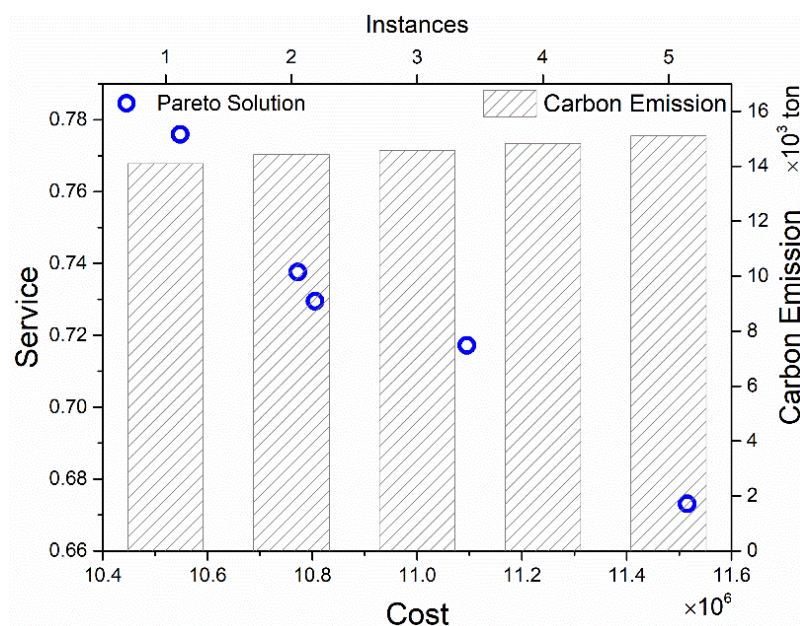

Figure 9. Pareto solutions and carbon emissions under different shipping routes.

Figure 10 also shows a similar pattern as Figure 8, that there is a difference between two speeds inside and outside the ECA. The ECA and non-ECA sailing speeds both increase with the distance inside ECA decreasing, which means cheaper fuel will be used along the route. When a ship sails a shorter distance inside the ECA and a longer total distance, the fuel consumption and carbon emissions increase with the sailing speed and total distance rising, whilst the fuel cost decreases due to less MGO used.

It can also be observed from the Pareto solutions in Figure 9, as expected, that the average service level of ports decreases with the total cost increasing. The service reliability of schedule design increases by 10% comparing Option 0 with the longest ECA distance and Option 4 with the shortest ECA distance, which reflects that ECA regulations may harm shipping service reliability and impact schedule operating when imposing emission

constraints. In addition, the carbon emissions are increasing with the ratio of ECA distance to total distance decreasing under different scenarios, which evidences the necessity of bringing ECA regulations into force.
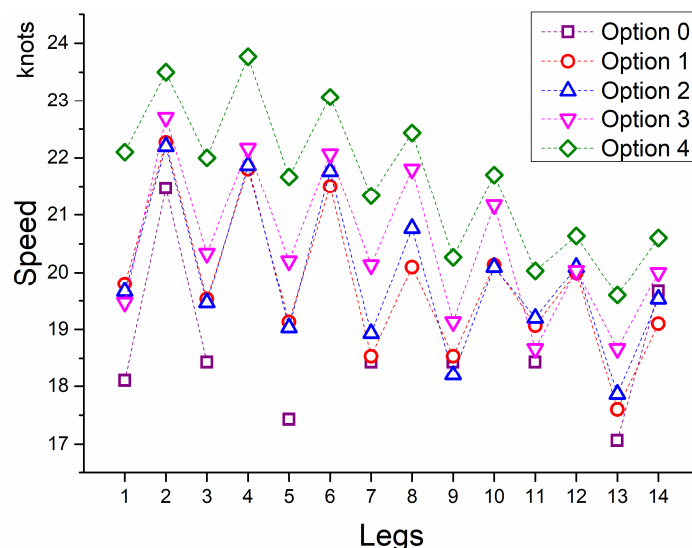

Figure 10. Average speed on each leg under different shipping routes.

6. Conclusions and Future Research

With the consistently growing attention paid from society to environmental benefits, the shipping industry is being called to put forward innovative approaches to improve the energy performance of ships in operation management. This paper aims to investigate how such regulations, mainly involving sulfur control within an ECA, impact green vessel scheduling (i.e., ship carbon emissions). Given that apparent viewpoint of the influence, it is highlighted that we address how to optimize two objectives, including the cost and the service unreliability, which have conflicting behavior. A novel bi-objective model has been presented and tackled by utilizing the augmented ε-constraint approach to produce a set of Pareto solutions by balancing the economic and environmental sustainability, which not only introduces ECA regulations but also captures robust weather conditions at sea and fuzzy port times. This would enable shipping lines to make appropriate decisions to satisfy their different preferences.

On the experimental aspect, almost all the instances are verified to be solved, and the results demonstrate a few interesting observations: (i) the UAM (upper approximation model) and LAM (lower approximation model) results obtained through the ME measure provide decisionmakers interval solutions with more information; e.g., by increasing the service level 3%, the total cost decreases from USD $12,606K$ to USD $108,966K$ when comparing the UAM and LAM results $\left(\sigma_{pk} = 0.7 \ \& \ \rho = 0\right)$; (ii) the weather impact in one month is very limited, while the incorporation of strong robustness against various weather conditions under different seasons is costly, both regarding fuel cost and service level; (iii) the fuzzy handling volume incurs changes in port time, and, if there is an increase in port time, this may further cause loss both in total cost and service reliability; (iv) LNG as a substitute fuel may acquire higher energy efficiency of ships when the bunker has a relatively low price, and vice versa; and (v) ECA regulations may harm service efficiency involving longer sailing distances inside the ECA.

Referring to managerial thinking, the liner shipping company should consider the uncertainties at sea and ports, and also the ECA regulations when designing the shipping schedule. It is better to reserve robust time to meet the planned schedule because of possible disruptions at port and at sea, like severe weather and uncertain port times. LNG is a good choice as a substitute fuel to mitigate sulfur emissions. When the ship operators

sail and encounter severe weather on the sea, they will have better reverse robust time to meet their planned schedule. As expected, the liner shipping companies design and implementation of green vessel schedules may increase energy efficiency and consider significant operational disciplines like cargo transit time requirements [53]. Hence, with the regulations on ship emissions that the IMO publishes becoming increasingly strict, liner shipping companies should bind together innovative technical means with slow steaming to construct a green vessel schedule by balancing economic benefits, energy efficiency, and service reliability to their needs.

Further research avenues regarding the following aspects would be worthwhile. Firstly, it would be more useful to present a life-cycle assessment of vessel emissions because the emissions exist in the liquefaction process, even including the production upstream. Secondly, other types of alternative fuel options besides LNG, such as methanol, liquid hydrogen (LH2), and biodiesel, or ship electrification could be considered in model formulations, as well as corresponding constraints capturing availability and storage. Thirdly, additional rich case studies should be conducted to focus on more shipping routes across the ECA.

Author Contributions: Methodology, Y.-Q.Y.; Writing—original draft, X.W.; Writing—review & editing, Q.C.; Supervision, Y.-y.L. All authors have read and agreed to the published version of the manuscript.

Data Availability Statement: Data have been included in article/references.

Nomenclature

Sets

P	set of ports on the service route $p = 1, 2, \ldots, N$
K	set of voyages $k = 1, 2, \ldots, M$
S	set of speeds $\delta \in S$
Λ	set of the ship positions on the sea, inside or outside ECA $\lambda \in \Lambda$
L_p^λ	set of segments inside or outside ECA on the leg from port p to next port $l \in L_p^\lambda$ divided by different wave regions

Parameters

s	maximum planned sailing speed
f_s (ton/h)	fuel consumption per unit distance when a ship sails with planned speed
γ^{port}	fuel consumption in unit time at port
d_p^λ	distance inside ECA or outside ECA on the leg from port p to the next port
d_l	distance on the segment $l \in L_p^\lambda$
Δv_l	decrease in sailing speed on the segment $l \in L_p^\lambda$
Δ^δ	travelling time when a ship sails at speed $\delta \in S$ per unit distance
h_p	minimum handling volume at port p
h_{pk}	actual handling volume at port p on voyage k
r_p	handling rate at port p
$\tilde{\varsigma}_{pk}$	uncertain waiting time at port p on voyage k
f^λ	unit fuel price for different types of fuel used inside or outside ECA
e^λ	unit carbon emission tax inside or outside ECA
θ^λ	carbon emission factor for different types of fuel used inside or outside ECA
θ^{port}	The carbon emission factor of MDO/MGO at port
u^h	unit handling activities cost
u^o	The unit operating cost of a ship per day

Decision variables	
$v_{pk}^{\lambda\delta}$	1 if the vessel sails at δ inside ECA or outside ECA from port p to the next port on voyage k; 0 otherwise
τ_p	designed transit time from port p to the next port
T	journey time of a single round trip
n	quantity of vessels arranged on the shipping route
EAT_{pk}	expected arrival time at port p on voyage k
EDT_{pk}	expected departure time from port p to the next port on voyage k
A_{pk}	actual arriving time at port p on voyage k
D_{pk}	actual departure time at port p on voyage k
$t_{pk}^{sailing}$	sailing time from port p to the next port on voyage k, including sailing time within and outside ECA
t_{pk}^{port}	port staying time at port p on voyage k, including uncertain waiting time and operating time
γ_l^δ	fuel consumption for sailing at speed δ on segment $l \in L_p^\lambda$
w_{pk}	The service level at port p on voyage k
FC	fuel consumption cost in a period
EC	carbon emission tax in a period
OC	operating cost in a period
HC	handling activities cost in a period

References

1. IMO. *Third IMO Greenhouse Gas Study*; IMO: London, UK, 2014.
2. Wan, Z.; El Makhloufi, A.; Chen, Y.; Tang, J. Decarbonizing the international shipping industry: Solutions and policy recommendations. *Mar. Pollut. Bull.* **2018**, *126*, 428–435. [CrossRef] [PubMed]
3. Adamopoulos, A. IMO Agrees to Cut Emissions by at Least 50% by 2050. 2018. Available online: https://lloydslist. maritimeintelligence.informa.com/LL1122195/IMO-agrees-to-cut-emissions-by-at-least-50-by-2050 (accessed on 4 March 2020).
4. Psaraftis, H.N.; Kontovas, C.A. Speed models for energy-efficient maritime transportation: A taxonomy and survey. *Transp. Res. Part C Emerg. Technol.* **2013**, *26*, 331–351. [CrossRef]
5. Fagerholt, K.; Gausel, N.T.; Rakke, J.G.; Psaraftis, H.N. Maritime routing and speed optimization with emission control areas. *Transp. Res. Part C Emerg. Technol.* **2015**, *52*, 57–73. [CrossRef]
6. Golias, M.M.; Boile, M.; Theofanis, S. Berth scheduling by customer service differentiation: A multi-objective approach. *Transp. Res. Part E Logist. Transp. Rev.* **2009**, *45*, 878–892. [CrossRef]
7. Egan, C. Lengthy Delays for Mega-Ships at Ports in Americas. 2014. Available online: https://www.joc.com/maritime-news/ international-freight-shipping/lengthy-delays-mega-ships-portsamericas_20140812.html (accessed on 20 May 2020).
8. Drewry. Satisfaction Survey in Container Transport: Customers More Dissatisfied with the Service Quality of Ocean Carriers. Available online: https://www.drewry.co.uk/news/news/satisfaction-survey-in-container-transport-customers-more-dissatisfied-with-the-service-quality-of-ocean-carriers (accessed on 3 April 2020).
9. Wang, S.; Meng, Q. Liner ship route schedule design with sea contingency time and port time uncertainty. *Transp. Res. Part B Methodol.* **2012**, *46*, 615–633. [CrossRef]
10. Lee, C.Y.; Song, D.P. Ocean container transport in global supply chains: Overview and research opportunities. *Transp. Res. Part B Methodol.* **2017**, *95*, 442–474. [CrossRef]
11. Meng, Q.; Wang, S.A.A.; Andersson, H.; Thun, K. Containership Routing and Scheduling in Liner Shipping: Overview and Future Research Directions. *Transp. Sci.* **2014**, *48*, 265–280. [CrossRef]
12. Fagerholt, K.; Laporte, G.; Norstad, I. Reducing fuel emissions by optimizing speed on shipping routes. *J. Oper. Res. Soc.* **2010**, *61*, 523–529. [CrossRef]
13. Norstad, I.; Fagerholt, K.; Laporte, G. Tramp ship routing and scheduling with speed optimization. *Transp. Res. Part C Emerg. Technol.* **2011**, *19*, 853–865. [CrossRef]
14. Hvattum, L.; Norstad, I.; Fagerholt, K.; Laporte, G. Analysis of an exact algorithm for the vessel speed optimization problem. *Networks* **2013**, *62*, 132–135. [CrossRef]
15. Wang, S.; Meng, Q. Sailing speed optimization for container ships in a liner shipping network. *Transp. Res. Part E Logist. Transp. Rev.* **2012**, *48*, 701–714. [CrossRef]
16. Wang, S.; Alharbi, A.; Davy, P. Liner ship route schedule design with port time windows. *Transp. Res. Part C Emerg. Technol.* **2014**, *41*, 1–17. [CrossRef]
17. Alharbi, A.; Wang, S.; Davy, P. Schedule design for sustainable container supply chain networks with port time windows. *Adv. Eng. Inform.* **2015**, *29*, 322–331. [CrossRef]
18. Zheng, J.F.; Ma, Y.Q.; Ji, X.; Chen, J.H. Is the weekly service frequency constraint tight when optimizing ship speeds and fleet size for a liner shipping service? *Ocean. Coast. Manag.* **2021**, *212*, 105815. [CrossRef]

19. Wu, Y.W.; Huang, Y.D.; Wang, H.; Zhen, L. Nonlinear programming for fleet deployment, voyage planning and speed optimization in sustainable liner shipping. *Electron. Res. Arch.* **2022**, *31*, 147–168. [CrossRef]

20. Alex, F.J.; Tan, G.; Kyei, S.K.; Ansah, P.O.; Agyeman, P.K.; Fayzullayevich, J.V.; Olayode, I.O. Transmission of viruses and other pathogenic microorganisms via road dust: Emissions, characterization, health risks, and mitigation measures. *Atmos. Pollut. Res.* **2023**, *14*, 101642. [CrossRef]

21. Li, C.; Qi, X.T.; Song, D.P. Real-time schedule recovery in liner shipping service with regular uncertainties and disruption events. *Transp. Res. Part B Methodol.* **2016**, *93*, 762–788. [CrossRef]

22. Qi, X.; Song, D.P. Minimizing fuel emissions by optimizing vessel schedules in liner shipping with uncertain port times. *Transp. Res. Part E Logist. Transp. Rev.* **2012**, *48*, 863–880. [CrossRef]

23. Song, D.P.; Li, D.; Drake, P. Multi-objective optimization for planning liner shipping service with uncertain port times. *Transp. Res. Part E Logist. Transp. Rev.* **2015**, *84*, 1–22. [CrossRef]

24. Aydin, N.; Lee, H.; Mansouri, S.A. Speed Optimization and Bunkering in Liner Shipping in the Presence of Uncertain Service Times and Time Windows at Ports. *Eur. J. Oper. Res.* **2017**, *259*, 143–154. [CrossRef]

25. Dulebenets, M.A. Green vessel scheduling in liner shipping: Modeling carbon dioxide emission costs in sea and at ports of call. *Int. J. Transp. Sci. Technol.* **2018**, *7*, 26–44. [CrossRef]

26. Norlund, E.K.; Gribkovskaia, I.; Laporte, G. Supply vessel planning under cost, environment and robustness considerations. *Omega* **2015**, *57*, 271–281. [CrossRef]

27. Norlund, E.K.; Gribkovskaia, I. Environmental performance of speed optimization strategies in offshore supply vessel planning under weather uncertainty. *Transp. Res. Part D Transp. Environ.* **2017**, *57*, 10–22. [CrossRef]

28. Mulder, J.; Dekker, R. Designing robust liner shipping schedules: Optimizing recovery actions and buffer times. *Eur. J. Oper. Res.* **2019**, *272*, 132–146. [CrossRef]

29. Wen, X.; Ge, Y.E.; Yin, Y.; Zhong, M. Dynamic recovery actions in multi-objective liner shipping service with buffer times. *Proc. Inst. Civ. Eng. Marit. Eng.* **2022**, *175*, 46–62. [CrossRef]

30. Debnath, K.; Roy, S.K. Power partitioned neutral aggregation operators for T-spherical fuzzy sets: An application to H_2 refuelling site selection. *Expert Syst. Appl.* **2023**, *216*, 119470. [CrossRef]

31. Mondal, A.; Roy, S.K.; Pamucar, D. Regret-based three-way decision making with possibility dominance and SPA theory in incomplete information system. *Expert Syst. Appl.* **2023**, *211*, 118688. [CrossRef]

32. Fagerholt, K.; Psaraftis, H.N. On two speed optimization problems for ships that sail in and out of emission control areas. *Transp. Res. Part D Transp. Environ.* **2015**, *39*, 56–64. [CrossRef]

33. Gu, Y.; Wallace, S.W. Scrubber: A potentially overestimated compliance method for the Emission Control Areas: The importance of involving a ship's sailing pattern in the evaluation. *Transp. Res. Part D Transp. Environ.* **2017**, *55*, 51–66. [CrossRef]

34. Lindstad, H.; Sandaas, I.; Strømman, A.H. Assessment of cost as a function of abatement options in maritime emission control areas. *Transp. Res. Part D Transp. Environ.* **2015**, *38*, 41–48. [CrossRef]

35. Chang, Y.-T.; Park, H.K.; Lee, S.; Kim, E. Have emission control areas (ECAs) harmed port efficiency in Europe? *Transp. Res. Part D Transp. Environ.* **2018**, *58*, 39–53. [CrossRef]

36. Chen, L.; Yip, T.L.; Mou, J. Provision of Emission Control Area and the impact on shipping route choice and ship emissions. *Transp. Res. Part D Transp. Environ.* **2018**, *58*, 280–291. [CrossRef]

37. Zhen, L.; Hu, Z.; Yan, R.; Zhuge, D.; Wang, S. Route and speed optimization for liner ships under emission control polices. *Transp. Res. Part C Emerg. Technol.* **2020**, *110*, 330–345. [CrossRef]

38. Zhuge, D.; Wang, S.; Wang, D.Z. A joint liner ship path, speed and deployment problem under emission reduction measures. *Transp. Res. Part B Methodol.* **2021**, *144*, 155–173. [CrossRef]

39. National Marine Environmental Forecasting Center. Available online: https://www.nmefc.cn/ybfw/wave/Global (accessed on 8 August 2019).

40. Xu, J.; Zhou, X. Approximation based fuzzy multi-objective models with expected objectives and chance constraints: Application to earth-rock work allocation. *Inf. Sci.* **2013**, *238*, 75–95. [CrossRef]

41. Notteboom, T.E. The time factor in liner shipping services. *Marit. Econ. Logist.* **2006**, *8*, 19–39. [CrossRef]

42. Vernimmen, B.; Dullaert, W.; Egelen, S. Schedule Unreliability in Liner Shipping: Origins and Consequences for the Hinterland Supply Chain. *Marit. Econ. Logist.* **2007**, *9*, 193–213. [CrossRef]

43. Lee, H.; Aydin, N.; Choi, Y.; Lekhavat, S.; Irani, Z. A decision support system for vessel speed decision in maritime logistics using weather archive big data. *Comput. Oper. Res.* **2018**, *98*, 330–342. [CrossRef]

44. Xiang, X.; Liu, C.; Miao, L. A bi-objective robust model for berth allocation scheduling under uncertainty. *Transp. Res. Part E Logist. Transp. Rev.* **2017**, *106*, 294–319. [CrossRef]

45. Esmaili, M.; Amjady, N.; Shayanfar, H.A. Multi-objective congestion management by modified augmented epsilon-constraint method. *Appl. Energy* **2011**, *88*, 755–766. [CrossRef]

46. Torabi, S.A.; Hassini, E. An interactive possibilistic programming approach for multiple objective supply chain master planning. *Fuzzy Sets Syst.* **2008**, *159*, 193–214. [CrossRef]

47. Mavrotas, G. Effective implementation of the ε-constraint method in multi-objective mathematical programming problems. *Appl. Math. Comput.* **2009**, *213*, 455–465. [CrossRef]

48. BunkerIndex. Available online: http://www.bunkerindex.com/prices/europe.php (accessed on 10 August 2018).

49. Kontovas, C.; Psaraftis, H.N. Reduction of emissions along the maritime intermodal container chain: Operational models and policies. *Marit. Policy Manag.* **2011**, *38*, 451–469. [CrossRef]
50. Clarkson. Available online: https://sin.clarksons.net/Timeseries/Advanced (accessed on 10 August 2018).
51. Venturini, G.; Iris, C.; Kontovas, C.A.; Larsen, A. The multi-port berth allocation problem with speed optimization and emission considerations. *Transport. Res. Part D Transp. Environ.* **2017**, *54*, 142–159. [CrossRef]
52. Notteboom, T.E.; Vernimmen, B. The effect of high fuel costs on liner service configuration in container shipping. *J. Transp. Geogr.* **2009**, *17*, 325–337. [CrossRef]
53. Dulebenets, M.A. The green vessel scheduling problem with transit time requirements in a liner shipping route with Emission Control Areas. *Alex. Eng. J.* **2018**, *57*, 331–342. [CrossRef]